*Int. J. Solids Structures* Vol. 26, No. 2, pp. 185–198, 1990
Printed in Great Britain.

0020–7683/90 $3.00 + .00


# A COMBINED ANALYTIC–FINITE ELEMENT METHOD FOR ELASTIC SHELLS

DAN GIVOLI
Department of Aeronautical Engineering, Technion—Israel Institute of Technology, Haifa 32000, Israel

(*Received* 7 *November* 1988; *in revised form* 2 *March* 1989)

**Abstract**—A method is devised for the numerical analysis of structures that include semi-infinite circular cylindrical shells. The so-called "edge stiffness coefficients" of the cylinder are used to eliminate the semi-infinite domain. Only a small region is thus left for discretization. In this computational domain a finite element scheme is used, which incorporates transverse shear deformation. Numerical examples demonstrate the superiority of the suggested method to the standard one.

## 1. INTRODUCTION

It is well known that numerical methods are essential in the analysis of complex problems of shell-type structures. Notwithstanding, most researchers would prefer to use an analytic method whenever possible, namely when a simple enough problem is at hand. However, there are often cases in which a *small region* in the problem domain makes it impossible to find an analytic solution. The problem can "almost" be solved analytically in those cases, but not quite. One example is the problem of the intersection of a number of long cylindrical shells. Although most of the domain is "simple", the intersection region may be too complex for analytic treatment.

It is clear that the use of a standard numerical scheme, such as the finite element method, to solve this type of problem would be inefficient. It seems natural to take advantage of the "regularity" of most of the domain and to put the numerical effort in the small "irregular" domain only. One method that works in this fashion is the coupled boundary-element finite-element procedure (see e.g. Zienkiewicz *et al.*, 1977; Margulies, 1981). In this method the entire problem is approximated from the outset. The large regular region $D$ is represented by a finite number of fundamental solutions which are used as trial functions in conjunction with the boundary-element method, whereas the small irregular domain $\Omega$ is discretized by the finite-element method.

In Givoli and Keller (1989), a different approach is suggested. The original problem is replaced by an *equivalent* problem which is defined in the small irregular domain $\Omega$. Then the problem in $\Omega$ is solved using the finite-element method. Thus, the large domain $D$ is eliminated *exactly*, unlike in the coupled BE–FE method. The method devised in Givoli and Keller (1989) has been used to solve the reduced wave equation in Keller and Givoli (1989), and two-dimensional problems in elastostatics in Givoli (1988). Here we use the same procedure to solve problems involving semi-infinite or infinite circular cylindrical shells with asymmetric loading.

One application is again the analysis of the intersection of two or more long cylinders. All the cylinders can be eliminated, leaving only the geometrically complicated intersection region for the numerical scheme. Another example is that of an irregularly-shaped pressure vessel from which emerge a number of long pipes. In the current approach the discretization of the pipes is avoided.

The procedure suggested here is as follows. First we introduce an artificial boundary $\mathscr{B}$ which separates the irregular domain $\Omega$ from the regular semi-infinite domain $D$. Then, we find an exact relation between displacements and forces on $\mathscr{B}$ based on an analytic analysis in $D$. If $\mathbf{U}$ is a vector of displacement-type quantities and $\mathbf{Y}$ is a vector of force-type quantities, then we find a relation of the form

$$\mathbf{Y} = -\mathbf{M}\mathbf{U} \quad \text{on } \mathscr{B}$$

where $\mathbf{M}$ is a matrix operator. In Givoli and Keller (1989) we call $\mathbf{M}$ the *Dirichlet-to-Neumann map*, or the DtN map, because it maps the Dirichlet-type data $\mathbf{U}$ to the Neumann-type data $\mathbf{Y}$. If $\mathbf{U}^n$ and $\mathbf{Y}^n$ are the $n$-th Fourier coefficients of $\mathbf{U}$ and $\mathbf{Y}$ on $\mathscr{B}$, then the above relation can be reduced to

$$\mathbf{Y}^n = \mathbf{S}^n\mathbf{U}^n$$

where the matrix $\mathbf{S}^n$ is called the "edge stiffness matrix" in the shell literature, and its elements are called the "edge stiffness coefficients" (see e.g. Steele, 1965; Simmonds, 1966). This matrix $\mathbf{S}^n$ has been used in the past to match two analytic solutions of the shell equations. Here we use it to "match" an analytic solution with a numerical solution.

The next step is to use the DtN relation as a *boundary condition* on $\mathscr{B}$, thus introducing a problem in the small domain $\Omega$ which is equivalent to the original problem. Finally, this new problem in $\Omega$ is solved via the finite element method.

We note that the expressions given in Steele (1965) and Simmonds (1966) for the edge stiffness coefficients are based on an asymptotic analysis. Hence the DtN boundary condition is not exact in this case. However, the approximation being made here is asymptotic in nature, not of a discretization type as in the coupled BE–FE method. The discretization in the DtN method is performed one step later.

In Section 2 we discuss the shell theories to be used in $D$ and $\Omega$ and the consistency of the matching between them. In Section 3 we present the finite element formulation for the new problem in $\Omega$. Two possible DtN boundary conditions, based on the two edge stiffness matrices suggested by Steele (1965) and Simmonds (1966), are discussed in Section 4. Finally, we present some numerical results in Section 5.

## 2. SHELL THEORIES AND MATCHING

Most of the popular "displacement" finite element methods for shells account for *transverse shear deformation*. This is not only due to the significance of shear deformation effects in moderately thick shells, but mainly because the resulting formulation is $C^0$ and thus enables simple interpolation. The scheme we have chosen to use here is the "degenerated shell element" procedure discussed in Hughes (1987), which incorporates transverse shear deformation. The main assumptions of this formulation are that plane sections remain plane, that the shell is inextensible in the thickness direction, and the "plane stress" assumption. In the context of the flat plate problem the same assumptions constitute the Reissner–Mindlin theory. There are five degrees of freedom at each node: three orthogonal displacements and two rotations.

The DtN approach necessitates finding an analytic solution to a quite general problem. However, the solutions available in the literature for this problem are all based on much simpler shell theories than the one employed in our numerical scheme. In particular, they do not include shear deformation. A "consistent" way of dealing with the DtN method would be to use a numerical scheme and a DtN map which originate from the same shell theory. This means either to employ a finite element scheme based on a simple theory for which the DtN map is known, or preferably to find the DtN map for the analytically more complicated shear deformation theory. We leave this last challenge for future work. Here we choose to make use of already existing tools, namely to match the two solutions in spite of their different origins.

We assume that we are dealing only with *thin* shells, where the transverse shear deformation is negligible. Thus, the difference between the two shell theories is essentially eliminated. The main difficulty which remains when trying to force such a matching is the incompatibility in the number of boundary conditions needed in the two theories. In the shear deformation theory, *five* prescribed values are needed at any edge point. A free edge of a cylinder, for example, is characterized by the following conditions:

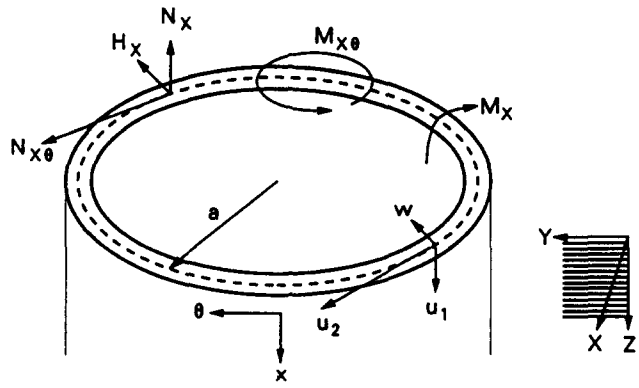


Fig. 1. Stress resultants, stress couples and displacements on the edge of a cylindrical shell.

$$N_x = N_{x\theta} = H_x = M_x = M_{x\theta} = 0. \tag{1}$$

Here $x$ is the axial coordinate and $\theta$ is the circumferential angle. The stress resultants $N_x$, $N_{x\theta}$, $H_x$, and stress couples $M_x$, $M_{x\theta}$ are described in Fig. 1. $N_x$ and $N_{x\theta}$ are normal and shear "membrane" forces, $H_x$ is a transverse shear force, and $M_x$ and $M_{x\theta}$ are bending and twisting moments. On the other hand, a theory which is based on the classic Kirchhoff–Love hypothesis (which does not include shear deformation) requires only *four* boundary conditions at each edge point. This is the outcome of the artificial reduction in the order of the equations which occurs when neglecting transverse shear terms. It is dictated by the mathematics, and one has to devise "effective" boundary conditions to replace the five "physically" required boundary conditions. For example, the effective free edge condition for a cylinder of radius $a$ is (see Timoshenko and Woinowsky-Krieger, 1959)

$$N_x = S_{x\theta} = T_x = M_x = 0 \tag{2}$$

where the effective forces $S_{x\theta}$ and $T_x$ are defined as

$$S_{x\theta} = N_{x\theta} + \frac{M_{x\theta}}{a} \tag{3}$$

$$T_x = H_x - \frac{\partial M_{x\theta}}{a\,\partial\theta}. \tag{4}$$

When we try to combine the numerical shear deformation scheme with an analytic solution based on the Kirchhoff–Love hypothesis we encounter a conflict between the number and characterization of the boundary conditions in the two cases. The simplest way out of this conflict is to assume $M_{x\theta} = 0$ on the DtN boundary, thus making $S_{x\theta}$ and $T_x$ equal to $N_{x\theta}$ and $H_x$, respectively, and identifying (1) with (2). In fact, this assumption is too strong. If $\chi_2$ is the "twist" rotation in the direction of $M_{x\theta}$ it suffices to assume that the product $M_{x\theta}\chi_2$ is negligible in comparison with other terms in the strain energy expression on the DtN boundary. That this assumption indeed resolves the conflict will be shown in Section 3.

Neglecting the "twist energy" is justified in many practical applications. For example, in problems involving the intersection of two pressurized cylinders the twisting moment is very small throughout the domain (see Steele and Steele, 1983). In other cases, the problem at hand can be solved *assuming* a small product $M_{x\theta}\chi_2$ on the DtN boundary. Then the validity of this assumption can be checked on the basis of the results. For instance, if the results show that $M_{x\theta}\chi_2$ is small *throughout* the domain then it is reasonable to accept the assumption as correct. A more general procedure would be to evaluate $M_{x\theta}\chi_2$ on the DtN

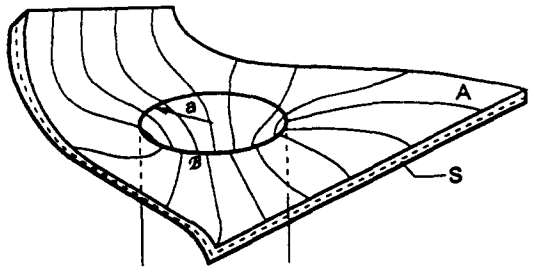


Fig. 2. A thin shell attached to a semi-infinite cylinder.

boundary from the numerical results, using equations of the Kirchhoff–Love-based shell theory which relate $M_{x\theta}$ and $\chi_2$ with other components, thus checking the assumption's consistency.

A different way to overcome the conflict in the computational scheme is to use special transition finite elements near the boundary $\mathscr{B}$ which possess the additional shear-deformation degrees of freedom on one side only.

## 3. FINITE ELEMENT FORMULATION

Figure 2 shows the midsurface $A$ of a shell attached to a semi-infinite cylinder along a circular artificial boundary $\mathscr{B}$ of radius $a$, along which the DtN boundary condition will be applied later. The external boundary of $A$ is denoted $S$. A differential element of the shell is described in Fig. 3, along with the stress resultants and couples acting on it. We use the lines-of-curvature curvilinear coordinates $\xi_1$ and $\xi_2$, and $\zeta$ is the coordinate perpendicular to the midsurface. Let $u_1$, $u_2$, $w$ be the displacements of a point of $A$ in the directions $\xi_1$, $\xi_2$, $\zeta$, and $\chi_1$, $\chi_2$ be the rotations about the $\xi_2$ and $(-\xi_1)$ coordinate axes, respectively. For simplicity, suppose that the edge $S$ is clamped, i.e. $u_1$, $u_2$, $w$, $\chi_1$ and $\chi_2$ are prescribed to be zero on $S$.

Defining the five "midsurface" strain measures $\varepsilon_{11}$, $\varepsilon_{22}$, $\varepsilon_{12}$, $\varepsilon_{31}$, $\varepsilon_{32}$, and the three "curvature" strain measures $\kappa_{11}$, $\kappa_{22}$, $\kappa_{12}$ in a standard way, we have the following variational form, or principle of virtual work (see Reddy, 1984):

$$0 = \int_A [\bar{\varepsilon}_{11}N_{11}+\bar{\varepsilon}_{22}N_{22}+\bar{\varepsilon}_{12}N_{12}+\bar{\kappa}_{11}M_{11}+\bar{\kappa}_{22}M_{22}+\bar{\kappa}_{12}M_{12}+\bar{\varepsilon}_{31}Q_1+\bar{\varepsilon}_{32}Q_2-\bar{w}\rho]\,\mathrm{d}A$$

$$-\int_{\mathscr{B}} [\bar{u}_1 N_{1n}+\bar{u}_2 N_{2n}+\bar{w}Q_n+\bar{\chi}_1 M_{1n}+\bar{\chi}_2 M_{2n}]\,\mathrm{d}\mathscr{B}. \quad (5)$$

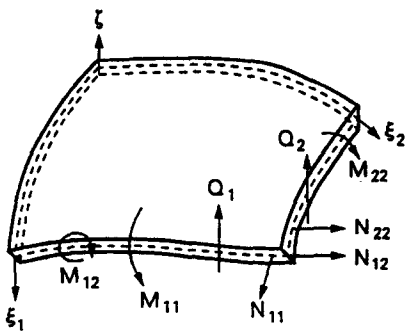


Fig. 3. A differential element of a thin shell, with stress resultants and stress couples.

The barred letters are weighting functions or "virtual" quantities, $p$ is the distributed lateral load, and a quantity $Z_n$ stands for $\sum_{\alpha=1}^{2} Z_\alpha n_\alpha$, where $\mathbf{n}$ is the normal unit vector pointing out of $S$. By applying the divergence theorem to (5) one obtains the corresponding "Euler–Lagrange" equations, in this case those of the shell theory which includes transverse shear deformation.

Equation (5) is not yet ready for the Galerkin approximation; we still have to impose the DtN boundary condition along $\mathscr{B}$. This involves the relation between the stress resultants and the displacements on $\mathscr{B}$. But as we have observed in Section 2 there are only four quantities of each kind in this relation, since it is obtained from a Kirchhoff–Love theory. Therefore, we are compelled to neglect the term $\bar{\chi}_2 M_{2n}$ in (5). In the equivalent problem of minimizing the potential energy functional this would correspond to neglecting the "twist energy" term $\chi_2 M_{2n}$. We also note that since $\mathscr{B}$ is actually the edge of a cylinder, we can identify $N_{1n}$, $N_{2n}$, $Q_n$, $M_{1n}$ and $M_{2n}$ along $\mathscr{B}$ with $N_x$, $N_{x\theta}$, $H_x$, $M_x$ and $M_{x\theta}$ of Fig. 1, respectively. Now, the DtN boundary condition is of the form

$$\mathbf{Y} = -\mathbf{M}\mathbf{U} \quad \text{on } \mathscr{B} \tag{6}$$

where

$$\mathbf{Y}^{\mathrm{T}} = \{N_x \quad N_{x\theta} \quad H_x \quad M_x\} \tag{7}$$

and

$$\mathbf{U}^{\mathrm{T}} = \{u_1 \quad u_2 \quad w \quad \chi_1\} \tag{8}$$

The DtN map $\mathbf{M}$ in (6) is a 4 by 4 matrix operator. Equation (6) can also be written in the more explicit form

$$\mathbf{Y}(\mathbf{x}) = -\int_{\mathscr{B}} \mathbf{m}(\mathbf{x}, \mathbf{x}')\mathbf{U}(\mathbf{x}')\, \mathrm{d}\mathbf{x}' \quad \mathbf{x} \in \mathscr{B} \tag{9}$$

where $\mathbf{m}(\mathbf{x}, \mathbf{x}')$ is called the DtN kernel. With (6) substituted into (5), the variational form becomes

$$\int_A [\bar{\varepsilon}_{11}N_{11} + \bar{\varepsilon}_{22}N_{22} + \bar{\varepsilon}_{12}N_{12} + \bar{\kappa}_{11}M_{11} + \bar{\kappa}_{22}M_{22} + \bar{\kappa}_{12}M_{12} + \bar{\varepsilon}_{31}Q_1 + \bar{\varepsilon}_{32}Q_2]\, \mathrm{d}A + \int_{\mathscr{B}} \bar{\mathbf{U}}^{\mathrm{T}}\mathbf{M}\mathbf{U}\, \mathrm{d}\mathscr{B} = \int_A \bar{w}p\, \mathrm{d}A. \tag{10}$$

This is the starting point for the finite element approximation. Equation (10) has the form

$$a(\bar{\mathbf{U}}, \mathbf{U}) + b(\bar{\mathbf{U}}, \mathbf{U}) = f(\bar{\mathbf{U}}, p) \tag{11}$$

where the operator $a(\cdot, \cdot)$ is the standard one, and

$$b(\bar{\mathbf{U}}, \mathbf{U}) = \int_{\mathscr{B}} \bar{\mathbf{U}}^{\mathrm{T}}\mathbf{M}\mathbf{U}\, \mathrm{d}\mathscr{B}. \tag{12}$$

The finite element scheme leads to the linear system of equations $\mathbf{K}\mathbf{d} = \mathbf{F}$. The operator $b(\cdot, \cdot)$ contributes to the stiffness matrix $\mathbf{K}$. We can write $\mathbf{K} = \mathbf{K}^a + \mathbf{K}^b$, where $\mathbf{K}^b$ is the contribution from the DtN boundary condition. The components of the DtN stiffness matrix $\mathbf{K}^b$ are

$$K^b_{AiBj} = b(N_A \mathbf{e}_i, N_B \mathbf{e}_j). \tag{13}$$

Here $N_A$ and $N_B$ are the finite element shape functions associated with nodes $A$ and $B$, and $i, j = 1, 2, 3, 4$ are the four degrees of freedom at nodes $A$ and $B$ on the boundary $\mathscr{B}$. The vector $\mathbf{e}_i$ has the value 1 as the $i$-th component and 0 for all the other components. The fifth degree of freedom ($i, j = 5$) does not contribute to $\mathbf{K}^b$ since it was suppressed in (10). Using (12) and the integral representation of $\mathbf{M}$ we find

$$K^b_{AiBj} = \int_{\mathscr{B}} \int_{\mathscr{B}} N_A(\mathbf{x}) m_{ij}(\mathbf{x}, \mathbf{x}') N_B(\mathbf{x}') \, d\mathbf{x} \, d\mathbf{x}'. \tag{14}$$

The construction of $\mathbf{K}^a$ and the right-hand side vector is described in detail in Hughes (1987). We mention that the formulation in this book employs a global Cartesian coordinate system $(X, Y, Z)$, and a transformation matrix $\mathbf{q}$ is used to transform quantities from it to the $(\xi_1, \xi_2, \zeta)$ system. A similar thing should be done with the DtN term if this global approach is desired. We denote $\mathbf{q}^*$ the transformation matrix from the local displacements $u_1$, $u_2$, $w$, $\chi_1$, to the global displacements $u_X$, $u_Y$, $u_Z$, $\chi_1$ (see Fig. 1). Thus,

$$\mathbf{U} = \begin{bmatrix} u_1 \\ u_2 \\ w \\ \chi_1 \end{bmatrix} = \mathbf{q}^* \begin{bmatrix} u_X \\ u_Y \\ u_Z \\ \chi_1 \end{bmatrix} \tag{15}$$

and

$$\mathbf{q}^* = \begin{bmatrix} 0 & 0 & 1 & 0 \\ -\sin\theta & \cos\theta & 0 & 0 \\ -\cos\theta & -\sin\theta & 0 & 0 \\ 0 & 0 & 0 & 1 \end{bmatrix}. \tag{16}$$

Then if $\mathbf{m}(\mathbf{x}, \mathbf{x}')$ still denotes the DtN kernel in the *cylindrical* system, (14) becomes

$$K^b_{AiBj} = \int_{\mathscr{B}} \int_{\mathscr{B}} N_A(\mathbf{x}) q^*_{ki}(\mathbf{x}) m_{kl}(\mathbf{x}, \mathbf{x}') q^*_{lj}(\mathbf{x}') N_B(\mathbf{x}') \, d\mathbf{x} \, d\mathbf{x}' \tag{17}$$

where the summation convention is in force.

We will see in the next section that $m_{ij}(\mathbf{x}, \mathbf{x}')$ can be written in the separable form

$$m_{ij}(\mathbf{x}, \mathbf{x}') = \sum_{n=0}^{\infty} S^n_{ij} \tilde{T}^n_i(\mathbf{x}) \tilde{T}^n_j(\mathbf{x}') \tag{18}$$

(no sum on $i$ and $j$). Noting that $d\mathbf{x} = a \, d\theta$ we finally have

$$K^b_{AiBj} = a^2 \sum_{n=0}^{\infty} \sum_{k=1}^{4} \sum_{l=1}^{4} S^n_{kl} \left( \int_0^{2\pi} N_A(\theta) q^*_{ki}(\theta) \tilde{T}^n_k(\theta) \, d\theta \right) \left( \int_0^{2\pi} N_B(\theta) q^*_{lj}(\theta) \tilde{T}^n_l(\theta) \, d\theta \right). \tag{19}$$

We see that only one-dimensional integrals need to be evaluated to account for the DtN contribution to the stiffness matrix.

If the semi-infinite cylinder is itself loaded (e.g. with uniform internal pressure), then the DtN map (6) becomes

$$\mathbf{Y} = -\mathbf{M}\mathbf{U} + \mathbf{Z} \quad \text{on } \mathscr{B} \tag{20}$$

where $\mathbf{Z}$ is a given vector function (although for uniform pressure $\mathbf{Z}$ is constant, i.e. does not depend on $\theta$). The variational form (10) has in this case an additional term in the right-hand side,

$$\text{R.H.S.} = \int_A \bar{w} p \, \mathrm{d}A + \int_{\mathscr{B}} \bar{\mathbf{U}}^{\mathrm{T}} \mathbf{Z} \, \mathrm{d}\mathscr{B} \tag{21}$$

which leads to the set of finite element equations

$$(\mathbf{K}^a + \mathbf{K}^b)\mathbf{d} = \mathbf{F}^a + \mathbf{F}^b. \tag{22}$$

Now $\mathbf{F}^b$ has the form

$$F^b_{Ai} = \int_{\mathscr{B}} N_A Z_i \, \mathrm{d}\mathscr{B} \tag{23}$$

in the shell coordinate system $(\xi_1, \xi_2, \zeta)$, or

$$F^b_{Ai} = \int_{\mathscr{B}} N_A \mathbf{e}_i^{\mathrm{T}} \mathbf{q}^* \mathbf{Z} \, \mathrm{d}\mathscr{B} \tag{24}$$

if the global coordinate system is used. The vector $\mathbf{Z}$ for uniform internal pressure will be given in the next section.

## 4. DtN BOUNDARY CONDITION

Throughout this section the summation convention will *not* be in force.

To derive the DtN map, we first write the components of $\mathbf{U}$ and $\mathbf{Y}$ in (7), (8) as Fourier series. To this end, we define the vectors of trigonometric functions $\mathbf{T}^n$ and $\hat{\mathbf{T}}^n$ as

$$(\mathbf{T}^n)^{\mathrm{T}} = \{\cos n\theta \quad \sin n\theta \quad \cos n\theta \quad \cos n\theta\} \tag{25}$$

$$(\hat{\mathbf{T}}^n)^{\mathrm{T}} = \{\sin n\theta \quad \cos n\theta \quad \sin n\theta \quad \sin n\theta\}. \tag{26}$$

This particular definition will lead to a greater symmetry in the equations that follow. Now we expand $\mathbf{Y}(\theta)$ and $\mathbf{U}(\theta)$:

$$Y_i(\theta) = \sum_{n=0}^{\infty} [Y_i^n T_i^n(\theta) + \hat{Y}_i^n \hat{T}_i^n(\theta)] \tag{27}$$

$$U_i(\theta) = \sum_{n=0}^{\infty} [U_i^n T_i^n(\theta) + \hat{U}_i^n \hat{T}_i^n(\theta)]. \tag{28}$$

Here $Y_i^n$, $\hat{Y}_i^n$, $U_i^n$, $\hat{U}_i^n$ are the Fourier coefficients. $Y_i^n$ and $U_i^n$ correspond to a symmetric configuration of the cylinder, whereas $\hat{Y}_i^n$ and $\hat{U}_i^n$ correspond to an antisymmetric configuration. There are some requirements concerning the $n = 0$ coefficients (namely $Y_1^0 = Y_2^0 = U_1^0 = U_2^0 = 0$) as well as inter-relations between the $n = 1$ coefficients so that the edge loads will be self-equilibrating and that rigid body displacements will be excluded. The Fourier coefficients of $U_i(\theta)$ can be written as

$$U_i^n = \frac{1}{\pi}\int_0^{2\pi} U_i(\theta)T_i^n(\theta)\,\mathrm{d}\theta; \qquad n \geqslant 1 \tag{29}$$

$$\hat{U}_i^n = \frac{1}{\pi}\int_0^{2\pi} U_i(\theta)\hat{T}_i^n(\theta)\,\mathrm{d}\theta; \qquad n \geqslant 1 \tag{30}$$

with a factor of $\frac{1}{2}$ on the right-hand side for $n = 0$.

Our goal is to express the DtN map in terms of the relation between the *Fourier coefficients* of **U** and **Y**. If we denote the vector containing $\{U_i^n\}_{i=1,2,3,4}$ by $\mathbf{U}^n$, etc., this relation can be written in the form

$$\mathbf{Y}^n = \mathbf{S}^n\mathbf{U}^n \tag{31}$$

$$\hat{\mathbf{Y}}^n = \hat{\mathbf{S}}^n\hat{\mathbf{U}}^n. \tag{32}$$

However, it is easy to show that $\mathbf{S}^n = \hat{\mathbf{S}}^n$. The matrix $\mathbf{S}^n$ is called the "edge stiffness matrix" in the shell literature, but we will refer to it as the DtN matrix. The derivation of $\mathbf{S}^n$ will be discussed shortly. In indicial notation (31) and (32) can be written as

$$Y_i^n = \sum_{j=1}^{4} S_{ij}^n U_j^n; \qquad \hat{Y}_i^n = \sum_{j=1}^{4} S_{ij}^n \hat{U}_j^n. \tag{33}$$

We now combine (27), (29), (30) and (33) to finally obtain

$$Y_i(\theta) = \frac{1}{\pi}\sum_{j=1}^{4}{\sum_{n=0}^{\infty}}' S_{ij}^n \int_0^{2\pi} [T_i^n(\theta)T_j^n(\theta') + \hat{T}_i^n(\theta)\hat{T}_j^n(\theta')]\, U_j(\theta')\,\mathrm{d}\theta' \tag{34}$$

where the prime in $\sum_{n=0}^{\infty}{}'$ signifies that a factor of $\frac{1}{2}$ should be taken for $n = 0$. Comparing (34) with (9) and noting that $\mathrm{d}x' = a\,\mathrm{d}\theta'$ we have the desired expression for the DtN kernel:

$$m_{ij}(\theta,\theta') = -\frac{1}{\pi a}{\sum_{n=0}^{\infty}}' S_{ij}^n[T_i^n(\theta)T_j^n(\theta') + \hat{T}_i^n(\theta)\hat{T}_j^n(\theta')]. \tag{35}$$

It remains to calculate the DtN matrix $\mathbf{S}^n$. The result will depend upon the specific shell theory dealt with, and is not easily obtained. Fortunately, this problem has been treated in the past. Here we consider the matrices suggested by Steele (1965) and by Simmonds (1966).

Steele's solution is based on an asymptotic analysis of Novozhilov's shell equations (1964). A distinction is made between "slow variation" and "rapid variation" behavior, for which two different asymptotic solutions are valid. Steele defines the "rapidness" parameter

$$\Omega = n\sqrt{\frac{c}{a}}. \tag{36}$$

Here $c$ is the reduced thickness of the cylinder, defined by $c^2 = t^2/12(1-\nu^2)$ where $t$ is the thickness and $\nu$ is the Poisson ratio. The graphs presented in Steele (1965) suggest that $\Omega = 0.5$ is a reasonable choice for the transition point from "slow variation" ($\Omega \ll 1$) to "rapid variation" ($\Omega \gg 1$) for a cylinder ($\lambda = 0$ in that paper). Let $E$ be Young's modulus and define $\Delta = (1+\nu)(3-\nu)$. Then after rescaling the displacement and force variables in Steele's paper as well as changing their order in the appropriate vectors, we obtain the following results for the DtN matrix:

For $\Omega \leqslant 0.5$,

$$\mathbf{S}^n = Et \begin{bmatrix} -\frac{\sqrt{2}\Omega^2}{\sqrt{ca}} & & & \\ -\frac{2(1-\nu)\Omega^3}{\sqrt{ca}} & -\frac{\sqrt{2}\Omega^2}{\sqrt{ca}} & & \\ \frac{(1-2\nu)\Omega^2}{a} & \frac{\sqrt{2}\Omega}{a} & -\frac{\sqrt{2c/a}}{a} & \\ -\sqrt{2}(1-\nu)\Omega^2\sqrt{c/a} & -\Omega\sqrt{c/a} & \frac{c}{a} & -\sqrt{2}c\sqrt{c/a} \end{bmatrix} \tag{37}$$

whereas for $\Omega \geqslant 0.5$,

$$\mathbf{S}^n = Et \begin{bmatrix} -\frac{2\Omega}{\Delta\sqrt{ca}} & & & \\ -\frac{(1-\nu)\Omega}{\Delta\sqrt{ca}} & -\frac{2\Omega}{\Delta\sqrt{ca}} & & \\ \frac{(1-2\nu)}{2\Delta a} & \frac{7+\nu}{4\Delta a} & -\frac{2\Omega^3\sqrt{c/a}}{a} & \\ -\frac{(1-\nu)\sqrt{c/a}}{4\Omega\Delta} & -\frac{\sqrt{c/a}}{2\Omega\Delta} & (1+\nu)\Omega^2\frac{c}{a} & -2\Omega c\sqrt{c/a} \end{bmatrix} \tag{38}$$

Due to the symmetry of these matrices, half of the off-diagonal terms are omitted.

It is shown by Steele that for the slowly varying case, the matrix (37) is singular or nearly singular. This might cause problems in other applications but not in the DtN method since we do not have to invert this matrix. We add the matrix $\mathbf{K}^b$ to the finite element stiffness matrix $\mathbf{K}^a$ which is already positive definite, and remains positive definite after this addition.

A second DtN matrix is given by Simmonds (1966), and is based on the asymptotic solution developed by Reissner and Simmonds (1966) to the extended Donnell equation. From the standpoint of the DtN method this solution has some disadvantages. First, it is algebraically more complicated than the former one. Second, only the "flexibility" matrix, i.e. the inverse of $\mathbf{S}^n$, is calculated by Simmonds. Third, in the "slowly varying" case the flexibility matrix is ill-conditioned, just as in Steele (1965), and its inverse must be computed in a special way (outlined in Simmonds, 1966). Nevertheless, this solution is also worth trying since it is based on an entirely different shell theory than that of Steele.

This time the "rapidness" parameter is defined as

$$\Omega^* = n^2\sqrt{\frac{2c}{a}} \tag{39}$$

and the suggested transition point between the solution for slow variation and rapid variation is $\Omega^* = 1$. The "flexibility" matrices $\mathbf{C}^n$ are given in Table 1 of Simmonds (1966) and will not be repeated here. To obtain the matrix $\mathbf{S}^n$ we have to invert $\mathbf{C}^n$ and to rescale and change the order of the variables. If we define

$$\mathbf{R} = \begin{bmatrix} 0 & 0 & 1 & 0 \\ 0 & 0 & 0 & a \\ 0 & 1 & 0 & 0 \\ 1 & 0 & 0 & 0 \end{bmatrix} \tag{40}$$

then

$$\mathbf{S}^n = \frac{Et}{a}\mathbf{R}^{\mathrm{T}}(\mathbf{C}^n)^{-1}\mathbf{R}. \tag{41}$$

There is an interesting interpretation of the zeroth term of the DtN map. For $n = 0$ the kernel $m_{ij}$ in (35) is the constant matrix

$$\mathbf{m}^0 = -\frac{1}{2\pi a}\begin{bmatrix} 0 & & & \text{symm.} \\ 0 & 0 & & \\ 0 & 0 & S^0_{33} & \\ 0 & 0 & S^0_{43} & S^0_{44} \end{bmatrix}, \tag{42}$$

which follows from the definitions (25), (26) as well as the structure of $\mathbf{S}^0$ in (37) when $\Omega = 0$. If we denote by $\mathbf{Y}^0$ the edge force vector obtained from the zeroth term only we then have from (9)

$$\mathbf{Y}^0 = \mathbf{S}^0\mathbf{U}^{\mathrm{AV}} \tag{43}$$

or in fact,

$$Y^0_1 = Y^0_2 = 0 \tag{44}$$

$$Y^0_i = S^0_{i3}U^{\mathrm{AV}}_3 + S^0_{i4}U^{\mathrm{AV}}_4; \quad i = 3,4 \tag{45}$$

where

$$U^{\mathrm{AV}}_i = \frac{1}{2\pi}\int_0^{2\pi} U_i(\theta)\,\mathrm{d}\theta \quad \text{on } \mathscr{B}. \tag{46}$$

Hence, the zeroth term in the DtN map relates the forces on the boundary with the *average* displacements on the boundary. If we use just this term as a boundary condition on $\mathscr{B}$ it means that we are assuming the edge forces to be *constant* and linearly dependent on the average displacements on $\mathscr{B}$ via the matrix $\mathbf{S}^0$. This is a better boundary condition than the one usually used to approximate long cylinders, namely that the edge forces (or the displacements) are *zero* along the artificial edge. Thus even if only the zeroth term is used, we can expect the DtN method to improve the finite element results.

We finally turn to the case when the semi-infinite cylinder is loaded with uniform internal pressure $q$. An expression for the vector $\mathbf{Z}$ in (20) is desired. From the superposition principle, this is the vector of edge forces corresponding to a *clamped* semi-infinite cylinder subjected to internal pressure $q$. The solution for such a cylinder is

$$\mathbf{Z}^{\mathrm{T}} = (N_x \quad N_{x\theta} \quad H_x \quad M_x) = q(0 \quad 0 \quad -\sqrt{2ac} \quad ac). \tag{47}$$

## 5. NUMERICAL EXPERIMENTS

We start with the example of an infinite cylindrical shell loaded with an external "ring" load $\cos 2\theta$; see Fig. 4(a). A solution to this problem is obtained in Niordson's book (1985), pp. 254–256. This is an *exact* (not asymptotic) solution to Morley–Koiter shell equations, and we will compare our results to it. The radius of the cylinder is $a = 1$, the thickness $t = 0.01$ and $E = 10^4$. Then Niordson's solution for the normal displacement $w_0$ under the load is

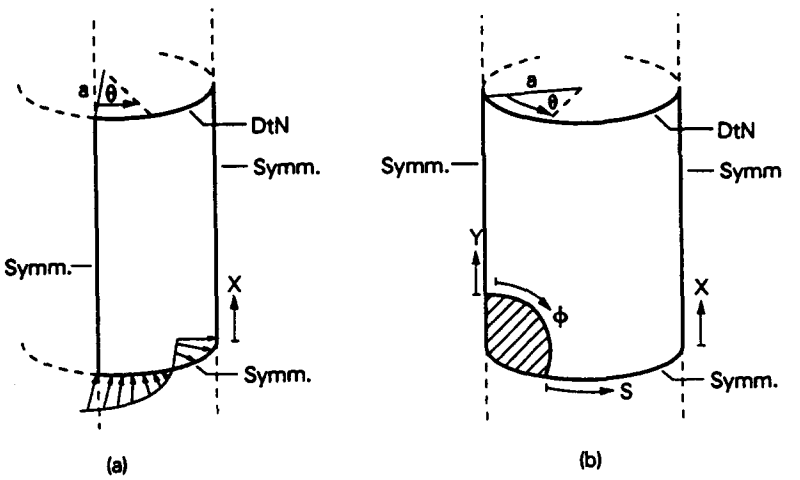


Fig. 4. Geometry of the two problems solved by the DtN method. (a) Infinite cylinder with a ring load. (b) Circular rigid inclusion in a pressurized infinite cylinder.

$$w_0(\theta) = \frac{0.01474}{2Etc^2}\cos 2\theta. \tag{48}$$

In the finite element scheme we take advantage of the symmetry by modeling only a *quarter* of the cylinder's circumference ($0 \leqslant \theta \leqslant \pi/2$) and only the portion of the cylinder on one side of the load ($x \geqslant 0$). Appropriate symmetry boundary conditions are imposed on the edges $\theta = 0$ and $\theta = \pi/2$, as well as on the edge $x = 0$, where only half of the load (i.e. $\frac{1}{2}\cos 2\theta$) is applied. An artificial boundary is introduced at $x = R = 0.3$. The mesh is rectangular and composed of 30 equal bilinear elements: 10 elements in the circumferential direction and three elements in the axial direction. The expected response has a boundary-layer nature, and the DtN approach avoids the discretization of most of this boundary layer. Thus only a few elements are needed, although they have to be small enough to capture the large gradients near $x = 0$.

In the standard finite element procedure we treat the artificial boundary as a free edge. Since the computational domain is a very narrow band near the loaded line, the finite element model is more similar to that of a *ring* than to that of an infinite cylinder. On the other hand, the DtN approach accounts for the whole cylinder through the DtN boundary condition.

Figure 5 shows some results for the normal deflection under the load along the arc $0 \leqslant \theta \leqslant \pi/4$. (The deflection along $\pi/4 \leqslant \theta \leqslant \pi/2$ is anti-symmetric to that shown.) The results obtained with Steele's DtN matrix and with Simmonds' DtN matrix are both shown, but cannot be distinguished in the plot. The difference between them is less than $\frac{1}{2}\%$. Both correspond very well with Niordson's solution. Since only the second term of the DtN map is active in this problem, this implies that the two matrices corresponding to $n = 2$ have an almost identical effect. In the free-edge finite element solution the deflection is overestimated to a great extent, as expected.

Before moving to the next example we note that the geometrical symmetry has two additional implications besides the ability to model only part of the shell structure. First, when imposing the DtN boundary condition the procedure outlined in Givoli and Keller (1989) must be applied. Second, the term $\hat{T}_i^n(\theta)\hat{T}_j^n(\theta')$ in the DtN kernel in (35) is not needed and can be disregarded. It corresponds to an *anti*-symmetric configuration, and thus would not contribute anything in (34) when the $U_j$ are symmetric displacements.

We now consider the problem of a circular rigid inclusion in a pressurized infinite cylinder, see Fig. 4(b). The cylinder is of radius $a = 10$, thickness $t = 0.2$, and is pressurized with $p = 1$. It is assumed to be open, i.e. no external axial load is applied. The rigid inclusion is of radius $r_0 = 3$. We also assume $E = 1$ and $\nu = 0.3$.

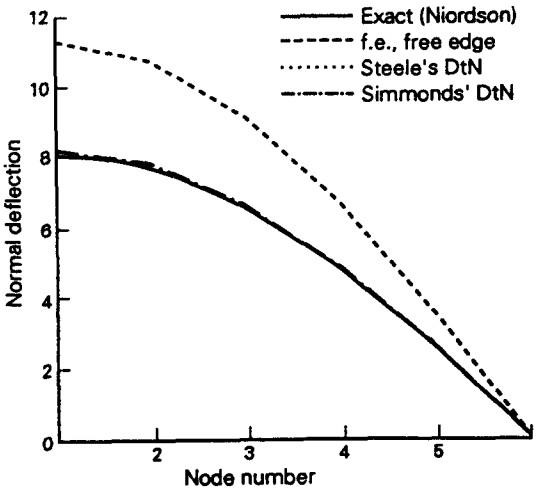


Fig. 5. The ring load problem: various solutions for the normal deflection under the load along the arc $0 \leqslant \theta \leqslant \pi/4$.

The cylinder is thin ($a/t = 50$) and the region near the inclusion can also be regarded as *shallow*, since $r_0/a = 3/10 < 0.5$. This enables us to compare our results with those obtained by Steele's code FAST2. See Steele and Steele (1983) and Steele (1983) for a description of the method and performance of the code. This program is intended to solve problems of nozzles in cylindrical vessels, but can be used to yield a solution for the problem of a circular rigid inclusion as a special case. The FAST2 solution cannot be regarded as the "exact solution" to our problem, but it will serve as a reference solution to compare our results to.

Here we model only half of the cylinder's circumference ($0 \leqslant \theta \leqslant \pi$) and only the portion $x \geqslant 0$, due to the symmetry. The artificial boundary is placed at $x = R = 7$. The "unfolded" mesh is described in Fig. 6, where bilinear quadrilateral elements are used. The left edge in the figure corresponds to $\theta = 0$ and the right edge to $\theta = \pi$. Appropriate symmetry boundary conditions are applied on these edges as well as on the lower edge, $x = 0$. The displacements and rotations of the nine nodes on the quarter circle which bounds the rigid inclusion are prescribed zero. The expected response is mainly of "membrane" type and the elements are therefore not required to be so small as in the previous example.

In the DtN approach, the DtN boundary condition is applied along the upper edge $x = 7$. Since the eliminated semi-infinite cylinder is uniformly pressurized, we include the right-hand side DtN contribution (24) in the load vector **F**, with the vector **Z** defined by (47). In the standard finite element scheme we choose a "mixed" boundary condition on that edge: we prescribe zero stress resultants $H_x$ and $N_{x\theta}$, zero axial displacement $u$ and zero rotations, $\chi_1$ and $\chi_2$.

In addition to the coordinate system $(x, \theta)$ it is convenient to introduce the polar system $(r, \phi)$, with its origin in the inclusion's center. We also define $s$ and $y$ to be the distances from the interface along the lines $x = 0$ and $\theta = 0$, respectively; see Fig. 4(b).

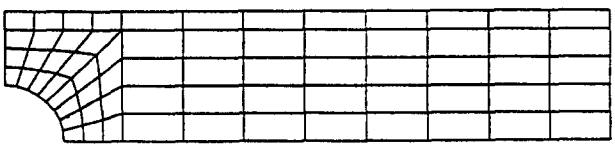

Fig. 6. Mesh for the circular inclusion problem.

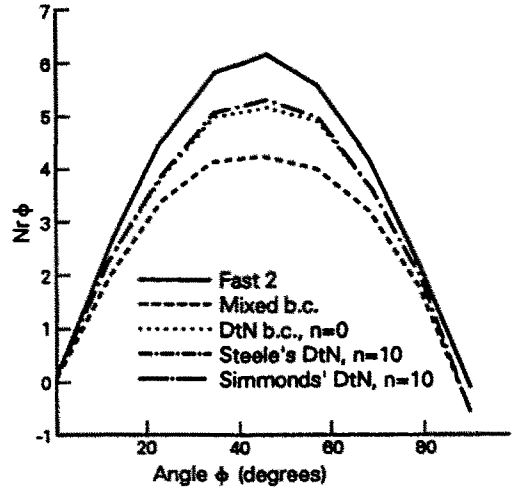


Fig. 7. The circular inclusion problem: various solutions for $N_{r\phi}$ around the inclusion boundary.

Figure 7 shows the results for the membrane shear stress resultant $N_{r\phi}$ around the boundary of the inclusion. To obtain it from stress resultants given in the $(x, \theta)$ coordinate system we use the tensorial transformation formula

$$N_{r\phi} = (N_\theta - N_x)\cos\phi\sin\phi + N_{x\theta}(\cos^2\phi - \sin^2\phi). \tag{49}$$

The results are shown for $0 \leqslant \phi \leqslant 90°$, and are slightly asymmetric with respect to $\phi = 45°$ Three DtN solutions are presented. The first is based on the zeroth DtN term, which is identical in Steele's and Simmonds' DtN solutions. The second and third are based on Steele's and Simmonds' DtN matrices with $n = 10$. The result obtained by FAST2 is linearly interpolated at the nodes. Figure 7 shows that the three DtN solutions are much closer to the FAST2 solution than the standard finite element solution. The correspondence between FAST2 and the DtN solutions would even be better for a smaller inclusion, where the theory which FAST2 is based on is more accurate. We also see that the DtN solution with $n = 10$ is only slightly better than the one for $n = 0$, and that Steele's and Simmonds' DtN matrices give almost the same results. (Again they are at most $\frac{1}{2}$% apart.)

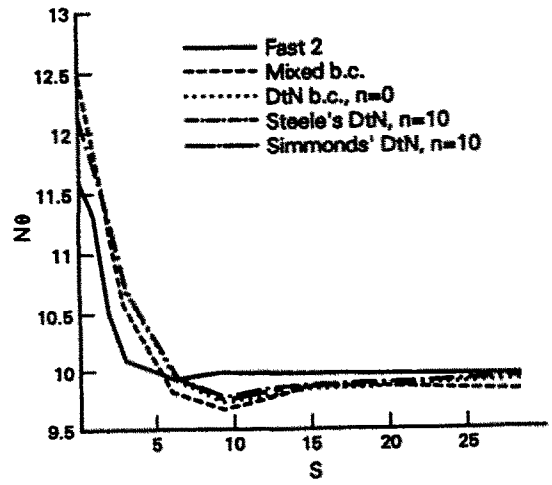


Fig. 8. The circular inclusion problem: various solutions for $N_\theta$ along the line $x = 0$.

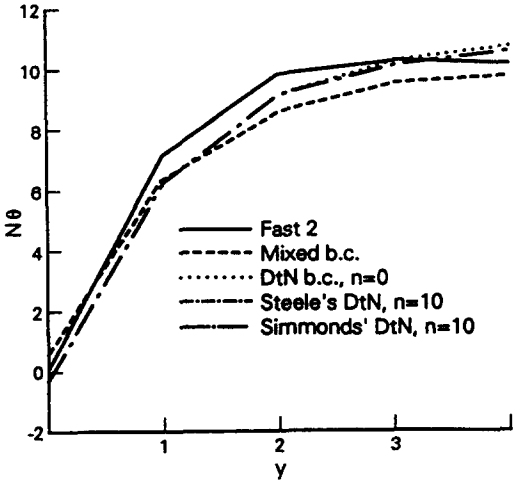


Fig. 9. The circular inclusion problem: various solutions for $N_\theta$ along the line $\theta = 0$.

In Fig. 8 some results for $N_\theta$ along the line $x = 0$ are compared, and Fig. 9 shows the results for $N_\theta$ along the line $\theta = 0$. The difference between the DtN and standard finite element solutions is less dramatic here, but in general the DtN solutions are closer to the FAST2 solution. Again, the three DtN solutions are very close to each other. Since Simmonds' DtN matrix is algebraically more complicated than Steele's matrix and they give practically the same results, it seems that the latter is preferable, at least for the type of problem dealt with here.

*Acknowledgements*—Part of this work was done at the Division of Applied Mechanics, Stanford University, California. The author is grateful to Prof. Joseph B. Keller for his help in the development of the ideas used here, and to Prof. Charles R. Steele for the opportunity to work with FAST2. At the Technion, the author is supported by the postdoctoral grant number 27000827.

## REFERENCES

Givoli, D. (1988). *A Combined Boundary Integral FE Method for Large Domain Problems, Boundary Elements X*, Vol. 1, 535–548. Springer, Southampton.

Givoli, D. and Keller, J. B. (1989). A finite element method for large domains. *Comp. Meth. Appl. Mech. Engng*, to appear.

Hughes, T. J. R. (1987). *The Finite Element Method.* Prentice-Hall, Englewood Cliffs, New Jersey.

Keller, J. B. and Givoli, D. (1989). Non-reflecting boundary conditions. *J. Comp. Phys.* **82**, 172–192.

Margulies, M. (1981). *Combination of Boundary Element and Finite Element Methods, Progress in Boundary Element Methods*, Vol. 1, 258–288. John Wiley, New York.

Niordson, F. I. (1985). *Shell Theory.* North-Holland, Amsterdam.

Novozhilov, V. V. (1964). *Thin Shell Theory.* Noordhoff, The Netherlands.

Reddy, J. N. (1984). *Energy and Variational Methods in Applied Mechanics.* John Wiley, New York.

Reissner, E. and Simmonds, J. G. (1966). Asymptotic solutions of boundary value problems for elastic semi-infinite circular cylindrical shells. *J. Math. Phys.* **45**, 1–22.

Simmonds, J. G. (1966). Influence coefficients for semi-infinite and infinite circular cylinderical elastic shells. *J. Math. Phys.* **45**, 127–149.

Steele, C. R. (1965). Shells with edge loads of rapid variation—II. *J. Appl. Mech.* **32**, *Trans. ASME series* **E87**, 87–98.

Steele, C. R. (1983). Comparison of FAST2 calculations with experimental results for thick and thin shells. *ASME Design Anal. Plates Shells* **105**, 45–53.

Steele, C. R. and Steele, M. L. (1983). Stress analysis of nozzles in cylindrical vessels with external load. *J. Pressure Vessel Technol.* **105**, 191–200.

Timoshenko, S. and Woinowsky-Krieger, S. (1959). *Theory of Plates and Shells.* McGraw-Hill, New York.

Zienkiewicz, O. C., Kelly, D. W. and Bettess, P. (1977). The coupling of the finite element method and boundary solution procedures. *Int. J. Num. Meth. Engng.* **11**, 355–375.